Molecular Nanomachines Disrupt Bacterial Cell Wall Increasing Sensitivity of Extensively Drug Resistant *Klebsiella pneumoniae* to Meropenem

Thushara Galbadage[1,#], Dongdong Liu[2], Robert Pal[7], James M. Tour[2,3,4,5,], Richard S. Gunasekera[2,6,8,#*], and Jeffrey D. Cirillo[1,*]*

[1]Department of Microbial Pathogenesis and Immunology, Texas A&M Health Science Center, Bryan, TX

[2]Department of Chemistry, [3]Department of Materials Science and NanoEngineering, [4]Smalley-Curl Institute, [5]NanoCarbon Center, [6]Department of BioSciences, Rice University, Houston, TX

[7]Department of Chemistry, Durham University, Durham, UK

[8]Department Biological Science, Biola University, La Mirada, CA

#Authors contributed equally

*Corresponding authors

E-mail: jdcirillo@tamu.edu, richard.gunasekera@biola.edu, tour@rice.edu

Abstract

Multidrug-resistance in pathogenic bacteria is an increasing problem in patient care and public health. Molecular nanomachines (MNM) have the ability to open cell membranes using nanomechanical action. We hypothesized that MNM could be used as antibacterial agents by drilling into bacterial cell walls and increasing susceptibility of drug resistant bacteria to recently ineffective antibiotics. We exposed extensively drug resistant *K. pneumoniae* to light-activated MNM and found that MNM increase susceptibility to meropenem. MNM with meropenem can effectively kill *K. pneumoniae* that are considered meropenem resistant. We examined the mechanisms of MNM action using permeability assays and transmission electron microscopy, finding that MNM disrupt the cell wall of extensively drug resistant *K. pneumoniae*, exposing the bacteria to meropenem. These observations suggest that MNM could be used to make conventional antibiotics more efficacious against multidrug-resistant pathogens.

Keywords: molecular nanomachines, nanomechanical action, light-activation, antimicrobial, antimicrobial resistance, multidrug resistance, extensively drug resistance.

Multidrug-resistant (MDR) pathogens are an increasing problem worldwide. Annually, 700,000 deaths are attributed to MDR and antimicrobial resistant (AMR) strains of common bacterial infections. This number, if current trends in the use of antibiotics continue, is projected to increase beyond 10 million annual deaths by 2050,.[1] MDR infections create an increasingly large burden in healthcare and preventative practices.[2] In their 2013 antibiotic-resistant threat report, the Centers for Disease Control and Prevention (CDC) listed 18 MDR and AMR pathogens that require immediate attention. Carbapenem-resistant Enterobacteriaceae (CRE) were identified as one of three pathogens at the highest threat level, demanding urgent action.[3] Recognizing the global impact of MDR and AMR pathogens on patient care, the World Health Organization (WHO) put forth a Global Action Plan (GAP) in 2015 to ensure continued success in effective treatment and prevention of these infectious diseases.[4] In 2017 WHO also identified CRE as one of three carbapenem-resistant pathogens in their highest priority category (Priority 1: Critical) for research and development of new antibiotics, again highlighting the urgent need for solutions to counter pathogens resistant to last resort antibiotics.[5]

Klebsiella pneumoniae belongs to the family of Enterobacteriaceae and is one of the most important causes of nosocomial infections worldwide.[6] This Gram-negative opportunistic pathogen colonizes the human intestine and is of high clinical importance, especially among very sick patients.[7] *K. pneumoniae* causes various healthcare-associated infections, including pneumonia, bloodstream infections, urinary tract infections, wound or surgical site infections, and meningitis.[8-10] Over the last few decades, MDR *K. pneumoniae* infections have rapidly increased in hospital settings, making first-line antibiotics vastly ineffective. The emergence of carbapenem-resistant strains of *K. pneumoniae* as a major nosocomial infection has raised many concerns as antibiotic treatment options available against this pathogen are very limited.[11-13] With the rapid

emergence of resistance to conventional antibiotics that were once considered wonder drugs, there is an emergent need for the development of new unconventional antibiotic agents that can effectively counter MDR pathogens.

Molecular nanomachines (MNM) are synthetic organic nanomolecules that have a rotor component with light-induced actuation (motorization) that rotates unidirectionally relative to a stator (Figure 1 a).[14-16] These MNM can disrupt synthetic lipid bilayers and cell membranes with their rapid rotational movement. Recently, ultraviolet light-activated MNM were shown to use nanomechanical action to drill into cell membranes, creating pores in targeted cancer cells and causing cell death.[17] Light-activated fast motor, MNM **1** (Figure 1 b) was shown to cause cell necrosis in human prostate adenocarcinoma cells (PC-3) and mouse embryonic fibroblast cells (NIH 3T3). MNM have various properties depended on their steric structure and attached functional groups. They can be modified to give them specific properties and functions. Light-activated MNM **1** rotates ~2-3 million revolutions per second and is considered a fast motor. Light-activated MNM **2** is a slow motor rotating only ~1.8 revolutions per hour and is a nanomechanical control for MNM **1**. MNM **3** is similar to MNM **1** but with a triphenylphosphonium (TPP) cation attached to its stator portion. TPP targets eukaryotic mitochondria causing MNM **3** to accumulate within mitochondria.[18] MNM can also have peptide appendages for specific cell adhesion. Nanomechanical action of fast motor MNM makes them potential broad-spectrum antibacterials. We hypothesized that MNM **1** can disrupt bacterial cell walls and act as a potent nanomechanical antibacterial agent either alone or facilitating the action of conventional antimicrobials.

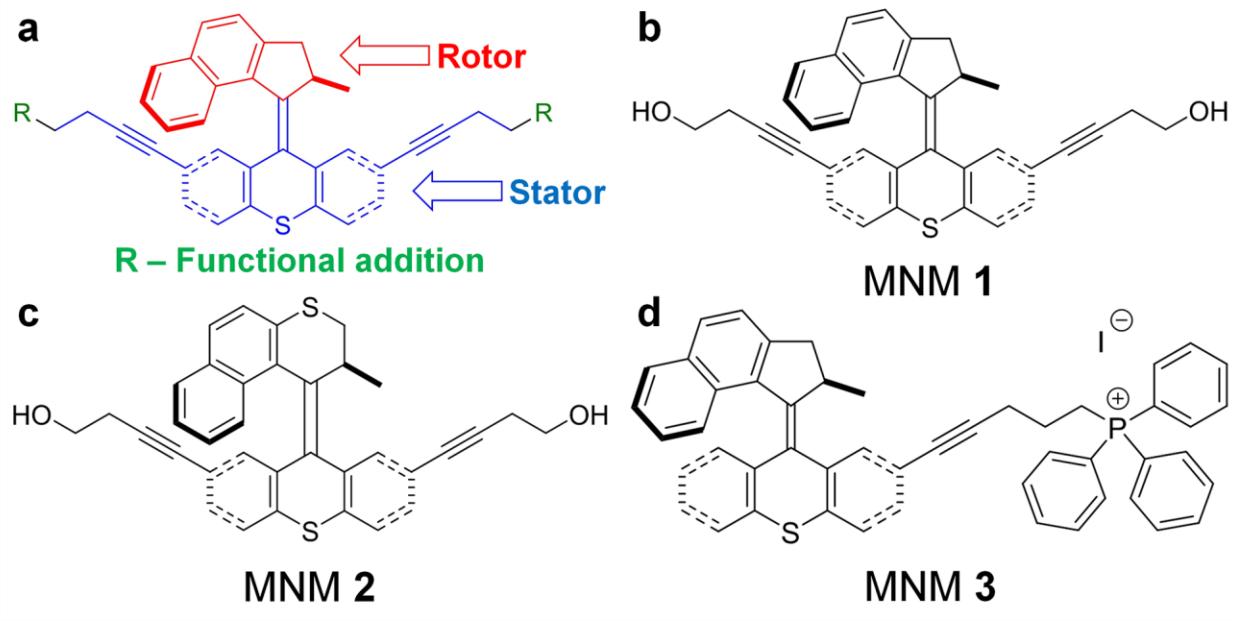

Figure 1. Molecular nanomachine (MNM) structures. (a) A representative MNM illustrating the rotor portions (red), which rotate upon light-activation relative to the stator portion (blue). R groups (green) are functional molecules that can be added to provide increased solubility, fluorophores for tracking or serve as recognition sites for cellular targeting. (b) MNM **1** is a fast motor with a unidirectional rotor activated by 365 nm light. (c) MNM **2** is the corresponding slow motor that serves as a control. (d) MNM **3** is a fast motor similar to MNM **1** but with a triphenylphosphonium (TPP) cation attached to the stator portion. TPP targets eukaryotic mitochondria causing MNM **3** to accumulate within mitochondria. This served as a control to demonstrate eukaryotic cell targeting of MNM.

Among various AMR mechanisms used by MDR *K. pneumoniae* to resist carbapenems, the loss of cell wall outer membrane porins and production of *K. pneumoniae* carbapenemase (KPC) confer the highest levels of carbapenem resistance.[19-22] The cell wall outer membrane (OM) lacking porins acts as a mechanical barrier that prevents carbapenem to permeate the OM and reach

its target site, penicillin-binding proteins (PBP) in the periplasmic space.[23] We explore the use of light-activated MNM **1** nanomechanical properties to drill pores and disrupt the cell wall in MDR *K. pneumoniae* to allow carbapenem to traverse the cell wall OM and cause bacterial cell death.

Here we use an extensively drug resistant (ψkp6) and an antibiotic sensitive (ψkp7) strain of *K. pneumoniae* to first show that light-activated MNM **1** using their nanomechanical action, can display antibacterial properties irrespective of pathogen antibiotic susceptibility profiles. Then we show that light-activated MNM **1** in combination with meropenem has the ability to make an extensively drug resistant *K. pneumoniae* susceptible to meropenem at sub-therapeutic concentrations. Our results indicate that light-activated MNM **1** uses its nanomechanical action to assist in bypassing the cell wall OM induced antibacterial resistance posed by *K. pneumoniae.* Thus, MNM **1** together with antibiotics like meropenem is shown as a potent antibacterial agent with the potential to effectively counter the increasing problem of multidrug resistance not only in *K. pneumoniae* but in many other MDR pathogens.

Results and Discussion

Characterization of optimum conditions for MNM light-activation against *K. pneumoniae*. The irradiance of the 365 nm LED light source (Sunlite Eagle 8WFP UV365 LED) used to activate the MNM was constant in the range of 10.5 to 12 mW/cm^2 measure over the course of 60 min at a constant distance (Figure 2 a). It had a narrow wavelength spectrum of 360 to 376 nm, with peak intensity at 368 nm (Figure 2 b). Any effects related to increase in heat due to the light source was excluded by the used of no MNM and slow MNM controls. Under these conditions, we assayed the bactericidal effects of the light source on an extensively drug-resistant *K. pneumoniae* (ψkp6) and an antibiotic sensitive *K. pneumoniae* (ψkp7). ψkp6 and ψkp7

antibiotics susceptibilities were characterized against several antibiotics using microdilution assays (Table 1). With 5 min of light exposure, we observed a viability reduction of 3% in ψkp6 and 6.5% in ψkp7. With 10 min of light exposure, it was 4% in ψkp6 and 18% in ψkp7, and at 60 min 40% in ψkp6 and 55% in ψkp7 (Figure 2 c). The overall bactericidal effects of 356 nm light on ψkp6 and ψkp7 were not significantly different (p=0.1802). Therefore a 5 min light-activation time was chosen to minimize the effects of 365 nm light on *K. pneumoniae*. For viability assays, 120 to 240 µL volumes of bacterial cultures were exposed to light directly placed above it at distance of 1.3 cm (Figure 2 d). For permeability and toxicity assays the light source was directly placed above the 96-well plate at a distance of 0.65 cm from the culture or media (Figure 2 e-f).

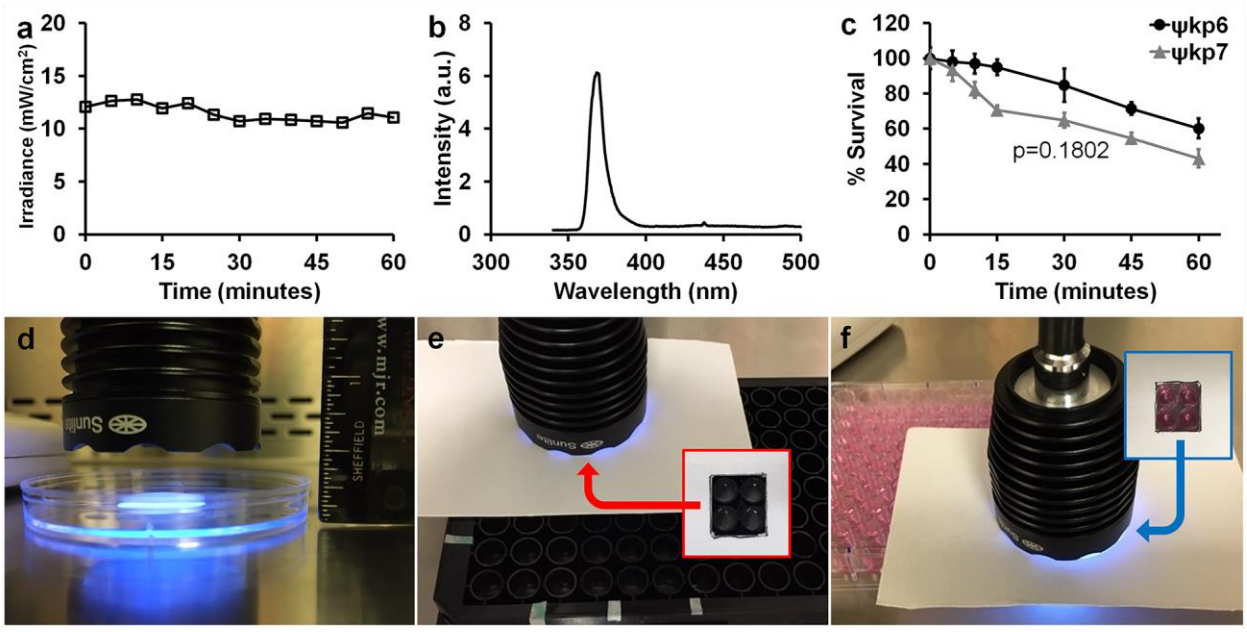

Figure 2. Characterization of 365 nm light source used to activate molecular nanomachines (MNM). (a) The irradiance of the 365 nm light source remained within a constant range of 10.5 to 12 mW/cm^2 measured over 1 h. (b) The range of wavelengths emitted by the 365 nm light source and their relative intensities with peak light intensity at 368 nm wavelength. (c) Bactericidal effect of the 365 nm light source on *K. pneumoniae* over 60 min of light exposure. ψkp6 (AR-0666), an

extensively drug-resistant strain of *K. pneumoniae.* ψkp7 (NIH-1), an antibiotic sensitive strain of *K. pneumoniae.* Percent survival was calculated by dividing the CFU/mL at each time point by the starting CFU/mL. A Mann-Whitney test was used to compare the survival of ψkp6 (AR-0666) and ψkp7 (NIH-1) strains (p=0.1802) (d) The light source placed directly above bacterial cultures at a constant distance of 1.3 cm for the duration of light exposure. (e-f) The light source placed directly above the 96-well plate to only expose four wells as shown by the inserts.

Table 1. Antibiotic susceptibilities of *K. pneumoniae* strains ψkp7 (NIH-1) and ψkp6 (AR-0666).

		ψkp7[a]			ψkp6[b]		
Antibiotic	Class	MIC[c] (μg/mL)	MBC_{99}[d] (μg/mL)	AST[e]	MIC (μg/mL)	MBC_{99} (μg/mL)	AST
Meropenem	Carbapenem	0.0625	0.0625	S(-)	16	16	R(+)
Tetracycline	Tetracycline	8	4	S(-)	256	256	R(+)
Gentamicin	Aminoglycoside	1	1	S(-)	> 512	> 512	R(+)
Amikacin	Aminoglycoside	1	1	S(-)	> 512	> 512	R(+)
Streptomycin	Aminoglycoside	4	4	S(-)	4	4	S(-)
Hygromycin	Aminoglycoside	64	64	S(-)	32	32	S(-)
Kanamycin	Aminoglycoside	2	2	S(-)	> 512	> 512	R(+)
Spectinomycin	Aminoglycoside	32	64	S(-)	64	> 512	R(+)
Rifampin	Rifamycins	32	32	R(+)	16	16	R(+)
Isoniazid	Isonicotinate	> 128	> 128	R(+)	> 128	> 128	R(+)

Ampicillin	Penicillin	> 512	> 512	R(+)	> 512	> 512	R(+)
Vancomycin	Glycopeptide	> 128	> 128	R(+)	> 128	> 128	R(+)

[a]ψkp7 strain (NIH-1), carbapenemase non-producing (KPC negative), antibiotic sensitive strain obtained from NIH.

[b]ψkp6 strain (AR-0666), carbapenemase producing (KPC positive), extensively drug-resistant strain obtained from the CDC.

[c]Minimal inhibitory concentration (MIC), the lowest concentration needed to inhibit bacterial growth determined by colony forming units (CFU).

[d]Minimal bactericidal concentration (MBC_{99}), the lowest concentration needed to kill 99% of the bacteria determined by CFU.

[e]Antibiotic susceptibility testing (AST): S(-) – sensitive, R(+) – resistant.

Light-activated MNM 1 cause reduced bacterial viability through its fast rotational movement in *K. pneumoniae*. To characterize the antibacterial properties of MNM **1,** we exposed the extensively drug-resistant (ψkp6) and the antibiotic sensitive (ψkp7) *K. pneumoniae* strains to 10 µM of MNM **1** (fast motor)**,** MNM **2** (slow motor) control and to the MNM solvent of 0.1% dimethyl sulfoxide (DMSO) control (no MNM), with 5 min of 365 nm light-activation (Figure 3 a). DMSO solvent was used so that the MNM remain soluble in media and DMSO at concentrations of 0.1% has no effects on cell viability.[17] The only significant reduction in CFU counts was observed in light-activated MNM **1** for both ψkp6 and ψkp7 ($p= 0.0219$ and 0.0078 respectively) (Figure 3 b-c). The percent viability reduction of ψkp6 exposed to light-activated MNM **1** was 21.3%, significantly higher than that of the no MNM (DMSO) control (5.4%) and MNM 2 control (4.6%) (Figure 3 b). Similarly, the percent viability reduction of ψkp7 exposed to

light-activated MNM **1** was 27.2%, significantly higher than that of the no MNM control (12.9%) and MNM 2 control (12.7%) (Figure 3 c). No toxicity or bactericidal effects were observed when 10 µM of non-light-activated MNM **1** was exposed to either ψkp6 or ψkp7. These results show that high-speed rotation of light-activated MNM **1** nanomechanical damage to *K. pneumoniae* irrespective of their antibiotic susceptibility, causing a significant relative reduction in viability (14-17%). In contrast, neither the light-activated MNM **2** nor the non-activated MNM **1** caused a significant reduction in viability. Our results showed no significant difference in the viability reduction observed in *K. pneumoniae* irrespective of their antibiotic sensitivity profiles. This suggests that antimicrobial resistance (AMR) mechanisms of this extensively-drug resistant strain have little or no effect on the nanomechanical action of light-activated MNM **1.**

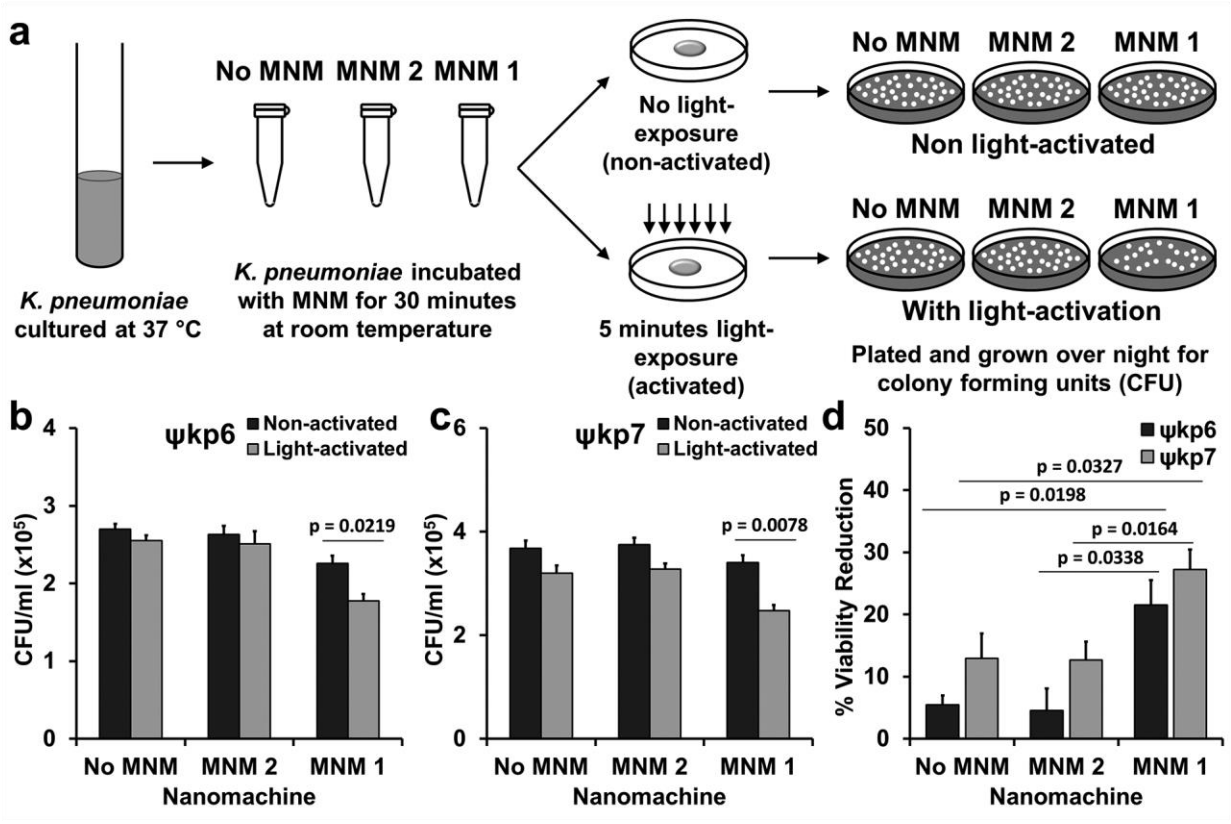

Figure 3. Viability reduction of *K. pneumoniae* with light-activated molecular nanomachines (MNM). (a) Experimental setup for bacterial viability reduction assays. A log growth phase culture

of *K. pneumoniae* incubated with no MNM (dimethyl sulfoxide (DMSO)), MNM **2** or MNM **1** for 30 min, activated with 365 nm light for 5 min and plated for CFU/mL counts. (b) An extensively drug-resistant strain of *K. pneumoniae* (ψkp6, AR-0666) exposed to no MNM (DMSO), 10 μM of MNM **2** or 10 μM of MNM **1**. Comparison of CFU/mL of *K. pneumoniae* after MNM exposure, without- and with-light activation. (c) An antibiotic sensitive strain of *K. pneumoniae* (ψkp7, NIH-1) exposed to no MNM (DMSO), 10 μM of MNM **2** or 10 μM of MNM **1**. Comparison of CFU/mL of *K. pneumoniae* after MNM exposure, without- and with-light activation. Results presented are means and standard error from four replicates for each group. p-values are from unpaired two-tailed Student t-test.

Light-activated MNM 1 causes cell wall inner and outer membrane disruptions in *K. pneumoniae*. To confirm the viability reduction observed in *K. pneumoniae* is a result of cell wall disruptions caused by the fast drilling action of light-activated MNM **1,** we carried out three assays to characterize the cell wall inner membrane permeability, outer membrane permeability, and cell membrane integrity. Cell wall inner membrane permeability of *K. pneumoniae* exposed to no MNM (DMSO control), 10 μM of MNM **2** or 10 μM of MNM **1** was determined using o-nitrophenyl-β-D-galactoside (ONPG), which is a substrate to cytoplasmic β-galactosidase that would leak through the cell wall inner membrane when disrupted. In both the extensively drug-resistant (ψkp6) and the antibiotic sensitive (ψkp7) *K. pneumoniae*, light-activated MNM **1** showed a significant increase in the β-galactosidase activity represented by an increase in absorbance at 410 nm wavelength (Figure 4 a-b). This was in contrast to both the light-activated MNM **2** and the non-activated MNM **1** that did not cause a significant increase in absorbance at 410 nm. To further characterize these differences, we calculated the differences in β-galactosidase activity at 30 min

post-exposure in Miller units.[24] In both ψkp6 and ψkp7, light-activated MNM **1** showed a significant increase in inner membrane permeability compared to non-activated MNM **1**, MNM **2** and no MNM (DMSO) control (Figure 4 c-d). These results indicate that upon light-activation, MNM **1** causes nanomechanical damage to *K. pneumoniae* cell wall inner membrane allowing the leakage of cytoplasmic β-galactosidase enzyme.

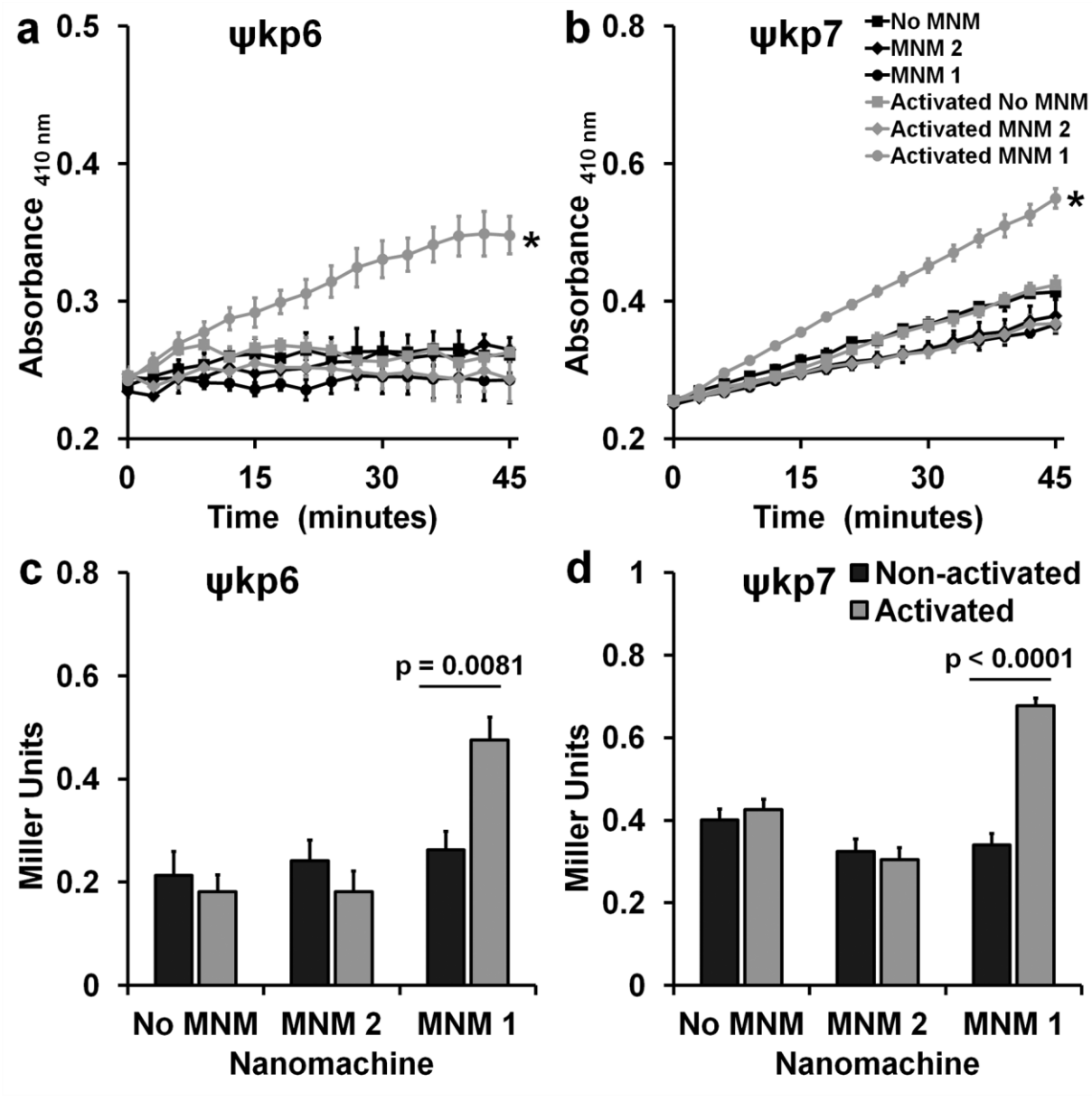

Figure 4. Cell wall inner membrane permeability with and without light-activation of molecular nanomachines (MNM). Cell wall inner membrane permeability of *K. pneumoniae* exposed to no MNM (DMSO), 10 μM of MNM **2** or 10 μM of MNM **1** determined by cytoplasmic β-galactosidase activity using o-nitrophenyl-β-D-galactoside (ONPG) as the substrate, measured with an increase in absorbance at 410 nm. (a,c) An extensively drug-resistant strain of *K. pneumoniae* (ψkp6, AR-0666) exposed to MNM. (a) Comparison in absorbance at 410 nm of *K. pneumoniae* with ONPG after MNM exposure, without- and with-light activation. (b,d) An antibiotic sensitive strain of *K. pneumoniae* (ψkp7, NIH-1) exposed to MNM. (b) Comparison in absorbance at 410 nm of *K. pneumoniae* with ONPG after MNM exposure, without- and with-light activation. (c-d) ONPG assay at 30 min with Miller calculation for inner membrane permeability of *K. pneumoniae* exposed to no MNM (DMSO control), 10 μM of MNM **2** or 10 μM of MNM **1**. Comparison of inner membrane permeability of *K. pneumoniae* after MNM exposure, without- and with-light activation. Results presented are means and standard error from four replicates for each group. (a-c) ***** $p<0.05$ are from a one-way ANOVA. (c-d) p-values are from unpaired two-tailed Student t-test.

We then studied the ability of light-activated MNM **1** to permeabilize the cell wall outer membrane using an *N*-phenyl-1-naphthylamine (NPN) uptake assay.[25] In both ψkp6 and ψkp7, light-activated MNM **1** showed a significant increase in NPN partitioning to the cell wall outer membrane represented by an increase in emission at 430 nm wavelength (Figure 5 a-b). This was in contrast to both the light-activated MNM **2** and the non-activated MNM **1** that did not cause a significant increase in emission at 430 nm. These results indicate that light-activated MNM **1** causes disruptions in the cell wall outer membrane allowing the uptake of NPN.

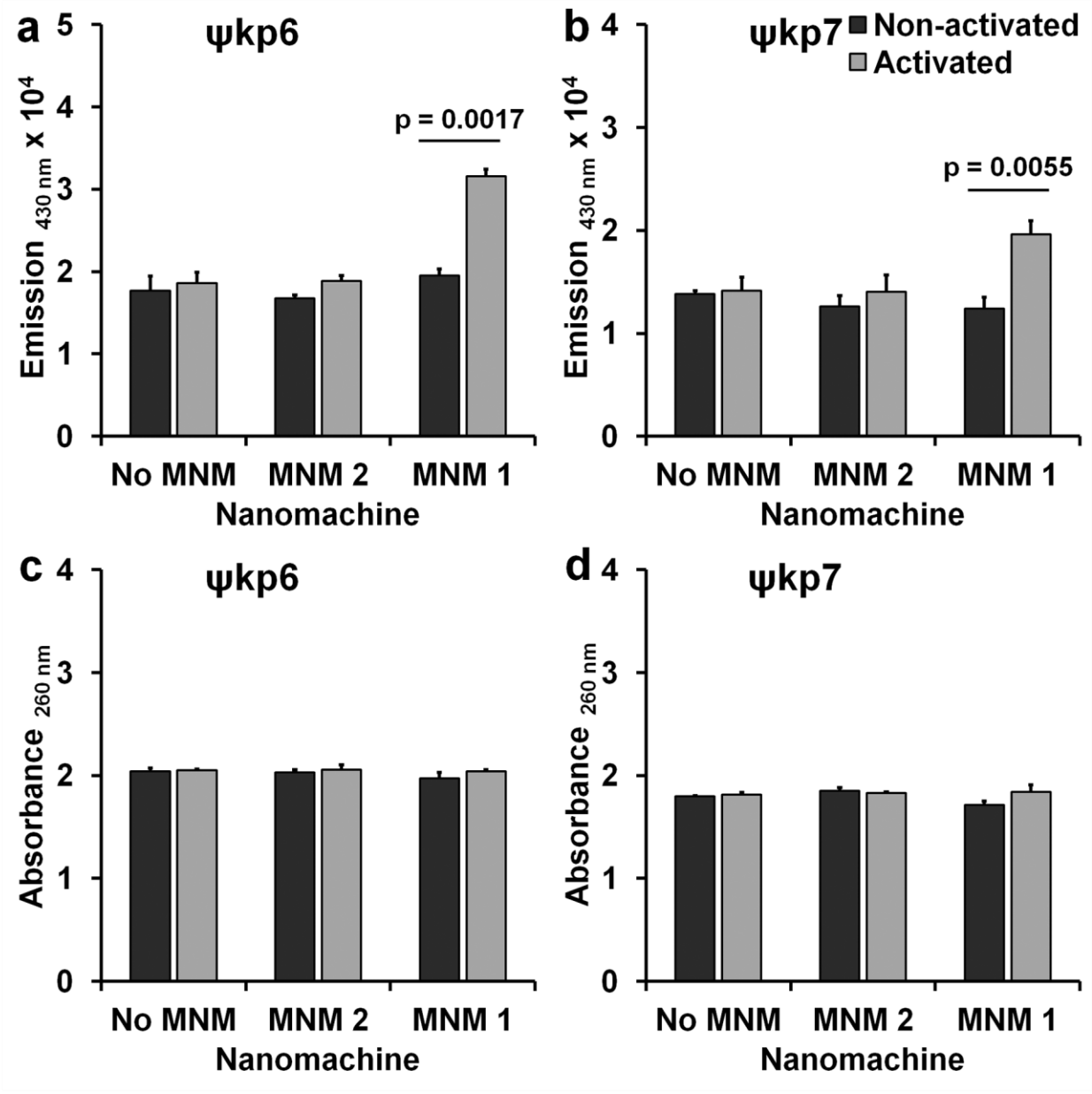

Figure 5. Cell wall outer membrane permeability and cell membrane integrity with and without light-activation of molecular nanomachines (MNM). (a-b) Cell wall outer membrane permeability assay of *K. pneumoniae* exposed to no MNM DMSO, 10 μM of MNM **2** or 10 μM of MNM **1**. Outer membrane permeability determined by the increase in fluorescence due to the partitioning of phenylnaphthylamine (NPN) into the cell wall outer membrane, measured by the increase in emission at 430 nm. Comparison of emission at 430 nm of *K. pneumoniae* with NPN

after MNM exposure, without- and with-light activation. (a) An extensively drug-resistant strain of *K. pneumoniae* (ψkp6, AR-0666) (b) An antibiotic sensitive strain of *K. pneumoniae* (ψkp7, NIH-1). (c-d) Cell membrane integrity assay of *K. pneumoniae* exposed to no MNM (DMSO), 10 μM of MNM **2** or 10 μM of MNM **1**. Disruptions in cell membrane integrity determined by cytoplasmic release of DNA and RNA, measured with an increase in absorbance at 260 nm. Comparison of absorbance at 260 nm of *K. pneumoniae* after MNM exposure, without- and with-light activation. (c) An extensively drug-resistant strain of *K. pneumoniae* (ψkp6). (d) An antibiotic sensitive strain of *K. pneumoniae* (ψkp7). Results presented are means and standard error from four replicates for each group. p-values are from unpaired two-tailed Student t-test.

To further characterize the extent of the cell wall damage caused by light-activated MNM **1**, we assayed the leakage of cytoplasmic constituents using absorbance at 260 nm that detect DNA and RNA in the supernatant.[26] Our studies showed that there was no significant difference in absorbance at 260 nm or relative changes with light-activated MNM **1**, MNM **2** or with no MNM control in both the *K. pneumoniae* strains ψkp6 and ψkp7 (Figure 5 c-d). These results indicate that cell membrane damage caused by light-activated MNM **1** was not large enough to allow the leakage of cytoplasmic DNA or RNA.

Our *K. pneumoniae* permeability assays indicate that light-activated MNM **1** is able to damage both the inner and outer membrane of the cell wall. This allowed smaller molecules such as enzymes and fluorescent dyes to cross the cell wall, but not larger molecules like DNA or RNA. The nanomechanical action of MNM **1** was not affected by antibiotic-resistant mechanisms since it caused cell wall damage to both *K. pneumoniae* strains alike.

Light-activated MNM 1 combined with meropenem to make an extensively drug resistant *K. pneumoniae* more sensitive to meropenem. Carbapenems are last resort antibiotics used in clinical settings against gram-negative pathogens. Carbapenem antibiotics cause bactericidal effects through penicillin-binding proteins (PBPs) with the inhibition of cell wall synthesis.[27] Loss of cell wall outer membrane porins is known to contribute to carbapenemase resistant in *K. pneumoniae* by acting as a physical barrier preventing carbapenem antibiotics reaching their target sites in the periplasmic space.[28] Since light-activated MNM **1** caused cell wall damage to *K. pneumoniae* irrespective of its antibiotic resistant profile, we hypothesized that MNM **1** will synergize with currently ineffective carbapenem antibiotics to make them more effective.

To test this hypothesis, we used light-activated MNM **1** with meropenem and tetracycline (control) at sub-therapeutic concentrations against the extensively drug resistant *K. pneumoniae* strain (ψkp6). In contrast to carbapenems, tetracycline antibiotics are protein synthesis inhibitors that prevent the initiation of translation by binding to the 30S ribosomal subunit.[29] We assayed meropenem at concentrations of 0.5 and 4 μg/mL, and tetracycline 16 and 128 μg/mL. These concentrations were lower than the MIC and MBC_{99} against ψkp6 (Table 1). Light-activated MNM **1** and meropenem at concentrations 0.5 and 4 μg/mL showed significant reduction in ψkp6 viability compared to non-activated MNM **1** with same concentrations of meropenem ($p=0.0455$ and 0.0095, respectively) (Figure 6 a). Light-activated MNM **1** and tetracycline at concentrations 16 and 128 μg/mL did not show a significant reduction in ψkp6 viability.

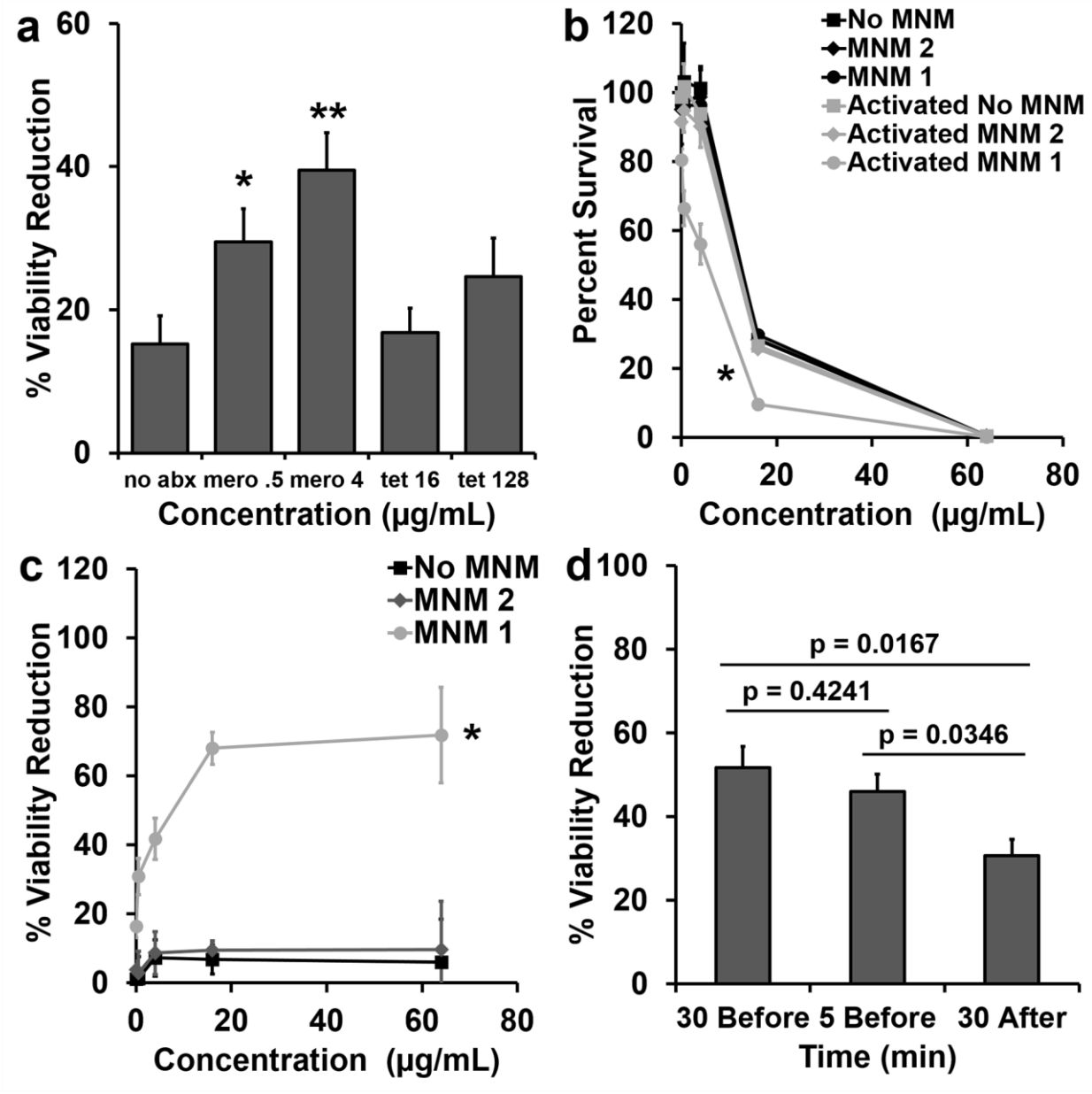

Figure 6. Viability reduction of *K. pneumoniae* with meropenem and light-activated molecular nanomachines (MNM). Viability reduction of extensively drug-resistant *K. pneumoniae* (ψkp6) exposed to antibiotics (meropenem or tetracycline), and no MNM (DMSO), 10 µM of MNM **2** or, 10 µM of MNM **1**. (a) Percent viability reduction of *K. pneumoniae* exposed to light-activated MNM with no antibiotics (no abx), 0.5 µg/mL meropenem (mero .5), 4 µg/mL meropenem (mero 4), 16 µg/mL tetracycline (tet 16), or 128 µg/mL tetracycline (tet 128). (b)

Percent survival of *K. pneumoniae* exposure to different concentrations of meropenem and MNM with or without light activation. (c) Percent viability reduction of light-activated no MNM, MNM **2** and MNM **1** compared to non-activated controls with different concentrations of meropenem (0.5 to 64 μg/mL). (d) Percent viability reduction of *K. pneumoniae* with light-activated MNM **1** with 4 μg/mL meropenem added 30 min before light-activation, 5 min before light-activation or 30 min after light-activation. Percent viability reduction was calculated by comparing light-activated groups with non-activated groups. Results presented are means and standard error from three replicates for each group. p-values are from unpaired two-tailed Student t-test, compared to no abx group. *, $p<0.05$. **, $p<0.01$.

When we used various doses of meropenem (0.5 to 64 μg/mL) in combination with 10 μM of light-activated MNM **1** to study the dose-depended combined effects of the combined therapy in reducing bacterial viability, as was expected, higher concentrations of meropenem alone showed increased reductions in viability, with 16 and 64 μg/mL of meropenem showing 70% and 98%, respectively (Figure 6 b). Without light-activation, MNM **1** or **2** did not have any additional viability reduction in *K. pneumoniae* (Figure 6 b). However, when MNM **1** was light-activated for 5 min in combination with meropenem, it caused a significant reduction in bacterial viability ($p<0.05$), shifting the survival curve to the left (Figure 6 b). At sub-therapeutic concentrations of meropenem (4 μg/mL), light-activated MNM **1** caused a 41.7% relative reduction in viability and at 64 μg/mL of meropenem, the relative reduction in viability was 72% (Figure 6 c). These results indicate that meropenem when combined with light-activated MNM **1** act to reduce bacterial viability in an extensively drug-resistant *K. pneumoniae* strain that is otherwise resistant to meropenem.

To further characterize the mechanism of interactions between meropenem and light-activated MNM **1**, we added meropenem 30 min before, 5 min before and 30 min after light activation. Our results show that the presence of meropenem during light-activation of MNM **1** showed higher viability reduction in ψkp6 (30 min before, 51.7% and 5 min before, 46.0%), compared to when added after light-activation (30 min after, 30.7%) (Figure 6 d). This suggests that there is a temporal relationship between meropenem and light-activated MNM **1**, and perhaps the cell wall damage or perturbation caused by MNM **1** is a transient effect. While we characterized the temporal aspect of the mechanistic relationship between meropenem and MNM **1,** it still needs more careful characterization. But the MNM alone, disrupting cell walls do result in bacterial death, albeit slower than in the presence of antibiotics.

Ultrastructural observations show light-activated MNM 1 and meropenem destroy extensively drug-resistant *K. pneumoniae*. To further confirm the combined action between light-activated MNM **1** and 4 μg/mL of meropenem, we exposed ψkp6 to MNM **1** with and without meropenem and light-activation and observed under transmission electron microscopy (TEM) (Figure 7). ψkp6 exposed to meropenem and non-activated MNM **1** showed minimal ultrastructural and morphological changes (Figure 7 a-d). In contract ψkp6 exposed to meropenem with light-activated MNM **1** showed distinct ultrastructural and morphological changes, many of which have been attributed to changes with meropenem (Figure 7 e-h).[30, 31] These observations included cell wall disruptions (yellow arrowhead), areas of clear cytoplasm (purple arrowhead), areas of cytoplasmic leakage (red arrowhead) and bacterial elongation. These observations were quantified in 60 to 80 ψkp6 per group (Figure 7 i and j). Compared to the control groups, ψkp6 exposed to light-activated MNM **1** and meropenem showed the presence to significantly higher cell wall disruptions, cytoplasmic clearance and cytoplasmic leakage ($P>0.005$) (Figure 7 i). The

extent of the ultrastructural damage caused was further quantified as mild, moderate and extensive. The light-activated MNM **1** and meropenem showed a significantly higher moderate and extensive ultrastructural damage in ψkp6 compared to the control groups (Figure 7 j). These TEM observations confirm our viability reduction results where light-activated MNM **1** made sub-therapeutic concentrations of meropenem effective against the extensively drug-resistant *K. pneumoniae* strain (ψkp6).

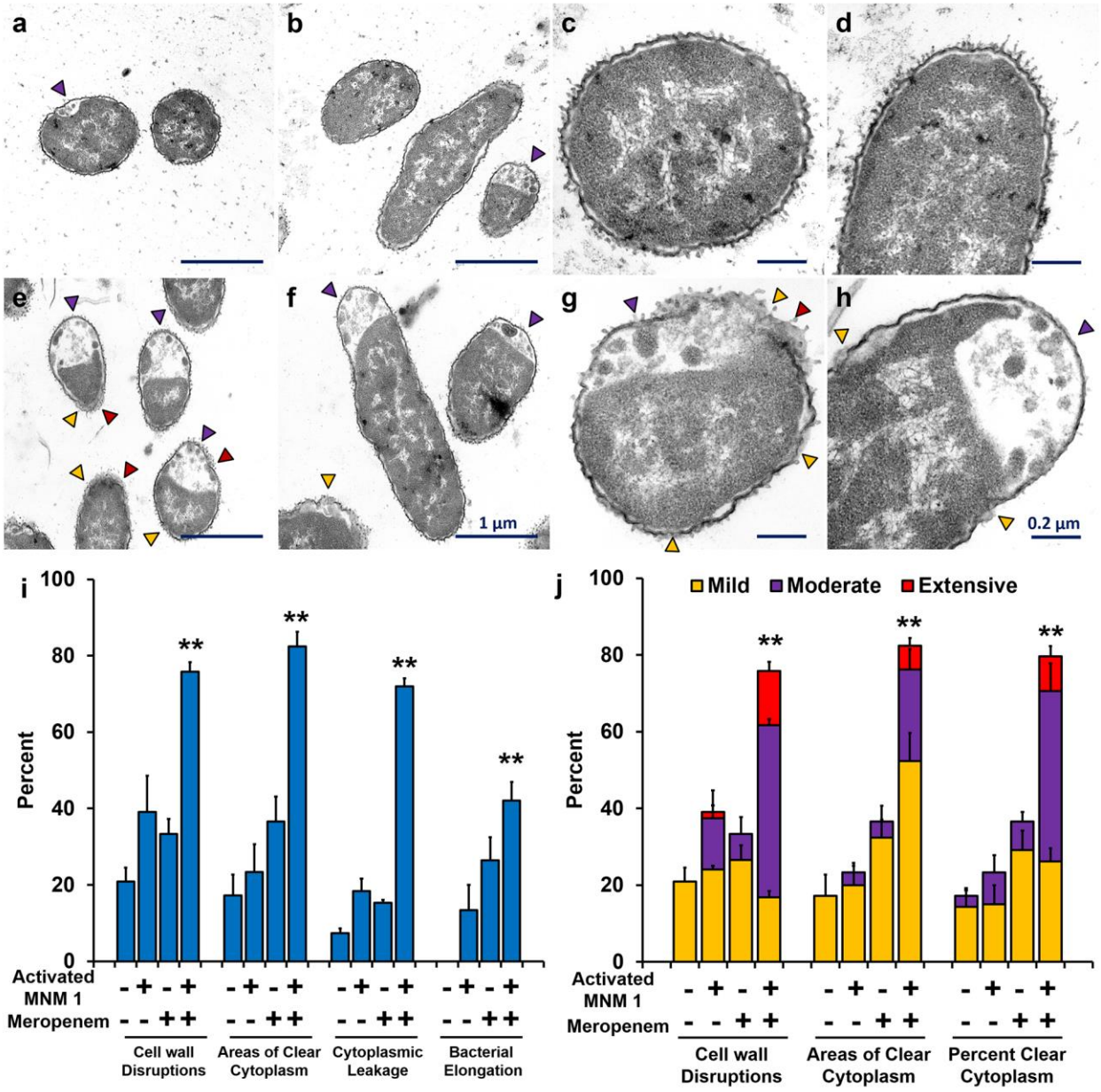

Figure 7. Cell wall disruptions and changes in *K. pneumoniae* exposed to meropenem and light-activated molecular nanomachines (MNM) observed through transmission electron microscopy (TEM). (a-d) Representative TEM images of *K. pneumoniae* incubated with 4 µg/mL meropenem and 10 µM of non-activated MNM **1** for 2.5 h. (e-h) Representative TEM images of *K. pneumoniae* incubated with 4 µg/mL meropenem and 10 µM of light-activated MNM **1** for 2.5 h (30 min prior to 5 min of 395 nm light-activation and 2 h post-light-activation). (a,e) Cross-section of bacilli at 20,000x magnification. (b,f) Longitudinal-section of bacilli at 20,000x magnification. (c,g) Cross-section of bacilli at 60,000x magnification. (d,h) Longitudinal-section of bacilli at 60,000x magnification. (a-h) Purple arrowheads show areas of cytoplasmic clearance. Yellow arrowheads show areas of cell wall disruptions. Red arrowheads show areas of cytoplasmic leakage. Scale bar for a-b, e-f is 1 µm. Scale bar for c-d, g-h is 0.2 µm. (i-j) Quantification of changes observed in 60 to 80 *K. pneumoniae* in each group with exposures to meropenem and MNM **1**. (i) Presence of cell wall disruptions ($p=0.0007$), areas of cytoplasmic clearance ($p=0.0002$), cytoplasmic leakage ($p<0.0001$) and bacterial elongation ($p=0.0022$) observed. (j) The degree of damage observed shown as mild, moderate or extensive for cell wall disruptions ($p=0.0004$), number of areas of clear cytoplasm ($p=0.0002$) and percent clear cytoplasm ($p=0.0003$). Results presented are the percentage of bacilli number in each exposure group. One-way ANOVA was used to compare the differences in means of each group. **, $p<0.01$.

We used TEM to confirm the combined action of light-activated MNM **1** with meropenem and showed that upon light-activation, the extensively drug resistant *K. pneumoniae* undergoes pathological and morphological changes such as cytoplasmic clearance and bacterial elongation that are associated with the action of meropenem. The significance of this finding is that light-

activated MNM **1** was able to make a sub-therapeutic concentration effective again. To study the mechanism of action between meropenem and MNM **1**, we examined the temporal effects of meropenem addition (Figure 7 i). We show that it is important that meropenem be present during light-activation MNM **1**, as the cell wall disruptions could be transient.

Light-activated MNM 1 does not cause cytotoxicity in J774A.1 macrophage cells. The use of a broad-spectrum nanomechanical antibiotic carries with it the concern of non-specific damage or associated cytotoxicity to adjacent host cells. To characterize the cytotoxic effects of light-activated MNM **1** (fast motor) on mammalian cells, we used J774A.1 macrophages and exposed them to various concentrations of MNM (0.5 to 100 µM) and observed them for up to 24 h post-exposure (Figure 8). We assayed 0.1 % DMSO (solvent) in media and MNM **2** (slow motor) as negative controls, and MNM **3** (fast motor with TPP, targeting mitochondria) as a positive control to perform an LDH cytotoxicity assay (Figure 8). At 24 h post-exposure, percent cytotoxicity observed were as follows: 1% DMSO without light-exposure = 1.8% and with light-exposure = 4.3% (Figure 8 a); 100 µM of MNM **1** without light-activation = 1.6% and with light-activation = 3.9% (Figure 8 b); 100 µM of MNM **2** without light-activation = 3.1% and with light-activation = 5.9% (Figure 8 c); and 100 µM of MNM **3** without light-activation = 76.5% and with light-activation = 87.2% (Figure 8 d). There was no statistical significance between non-activated MNM **1** and MNM **2** or no MNM (DMSO) control. This shows that even at a 10x concentration (100 µM) used against *K. pneumoniae*, MNM **1** does not display any cytotoxicity in macrophages. However, when exposed to light, both the no MNM (DMSO) control and MNM **1** showed an increase in cytotoxicity ($p<0.005$), showing the cytotoxic effects of 365 nm light on mammalian cells.

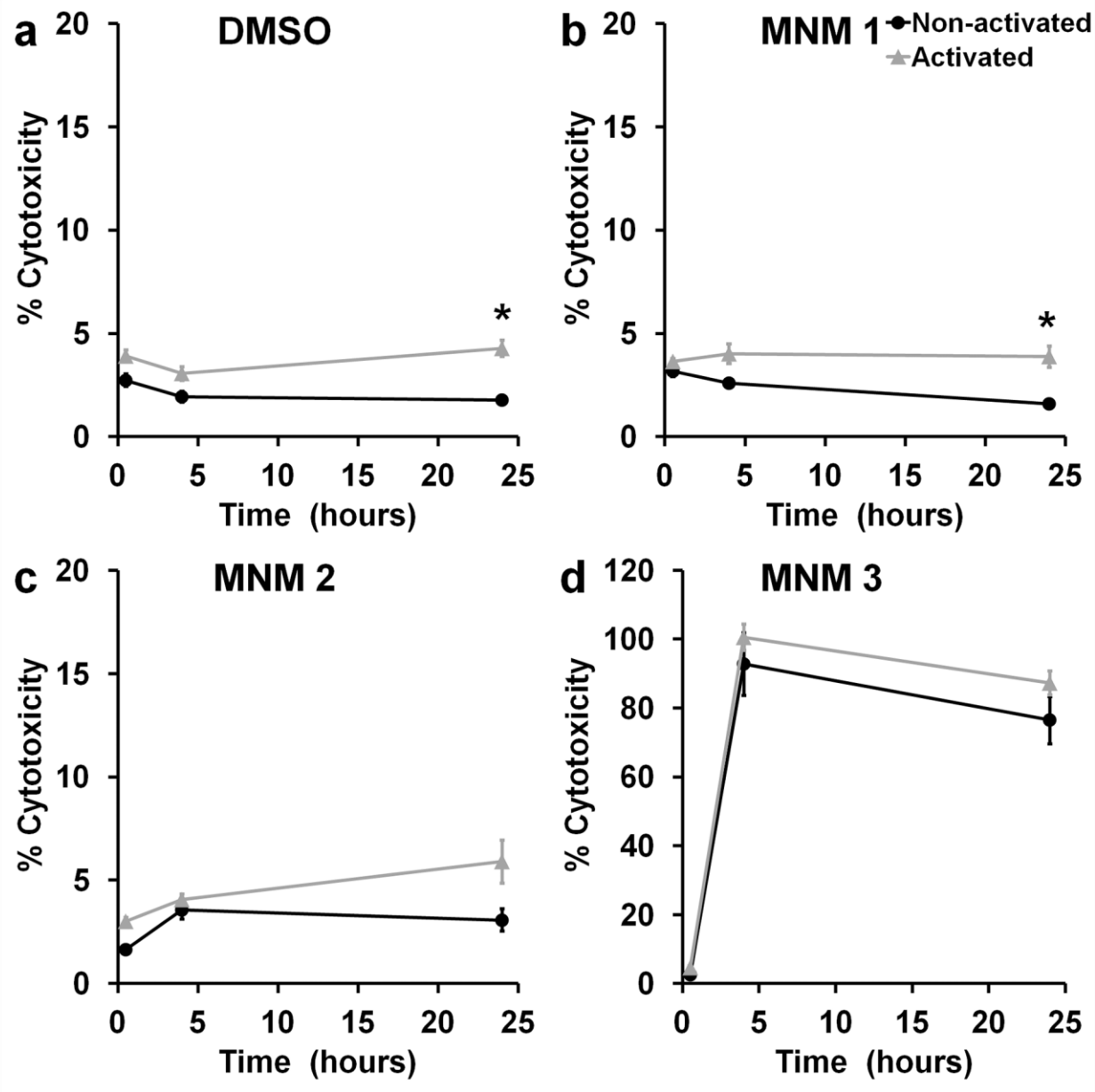

Figure 8. Cytotoxicity of molecular nanomachine (MNM) treatment for J774A.1 macrophages. Percent cytotoxicity of macrophage cells measured with an LDH assay at 0.5, 4 and 24 h exposed to 100 µM MNM without or with light-activation. Percent cytotoxicity was calculated using a low control (natural cell death) (0%) and a high control (triton-x induced cell death) (100%) (a) Without MNM (1% DMSO) (p=0.0282). (b) With 100 µM of MNM **1** (fast motor) in 1% DMSO (p=0.0428). (c) With 100 µM of MNM **2** (slow motor) in 1% DMSO

(p=0.1971). (d) With 100 μM of MNM **3** (fast motor with TPP, targeting mitochondria) in 1% DMSO (p=0.8748). The DMSO concentration was 1% because 100 μM MNM was assayed. Results presented are mean and standard error from four replicates. *, $p<0.05$.

Light-activated MNM 1 assists meropenem in killing an extensively drug-resistant *K. pneumoniae*. Meropenem-resistant *K. pneumoniae* uses different mechanisms to prevent meropenem from reaching PBP within peptidoglycan in the periplasmic space. One such resistant mechanism is a cell wall outer membrane lacking porins that keep meropenem out of the bacteria.[23] When MNM **1** is activated with 365 nm light, it rotates unidirectionally at 3 MHz to drill pores into the cell wall of *K. pneumoniae* through its nanomechanical action. These pores allow meropenem to travel across the cell wall outer membrane and reach PBP. This causes the destruction of the peptidoglycan layer, destabilizing the bacterial cell wall and leading to the death of *K. pneumoniae*. This synergistic mechanism between light-activated MNM **1** and meropenem allows sub-therapeutic concentrations of meropenem to kill meropenem resistant, extensively drug-resistant *K. pneumoniae*.

There are a few limitations in this study. MNM **1** has a non-specific action, without any specific binding affinity to *K. pneumoniae*. When MNM **1** was previously used to target and permeabilize cancer cells, they had short sequence peptides that allowed selective binding and high cell specificity. Targeting specific bacterial receptors using ligands can increase the specificity to the pathogen.[32] Several ligands including aGM1, aGM2, and GM2 have been shown to have specificity to *K. pneumoniae* and can be attached to the MNM stator to increase their specificity and efficacy.[33-35]

Another concern of the non-specific nature of MNM **1** is the toxicity and possible damage it can cause to surrounding host cells during light-activation. In order to address this issue, we looked at the cytotoxicity of MNM **1** in macrophages (Figure 8). We only observed a 1.6% cytotoxicity with 100 µM (10x more) MNM **1**. However, with 365 nm light-exposure, the macrophage cytotoxicity increased to 3.9-5.9% (p-value <0.05), highlighting the concerns with this use of 365 nm light. This also limited our MNM **1** activation time to 5 min since 365 nm light displayed higher bactericidal effects over longer exposure times (Figure 2 c). To address this, we are in the process of developing 405 nm light-activated MNM that will be safer and allow longer activation times.

A wavelength of 365 nm has relatively low penetration in host organs and tissue. This currently limits the use of MNM for the potential treatment of deep tissue infections, as MNM will not be activated effectively. We are also exploring the synthesis of next generation MNM that are activated with longer wavelengths (>700 nm) in the near infrared (NIR) region. This will greatly increase the ability of MNM activation in much deeper host targets and also allow the activation of MNM for longer times to achieve a far superior antimicrobial efficacy, without any associated harmful effects on the host. However, the energies at these wavelengths are much lower. We have been exploring 2-photon NIR, albeit the potential depth may be somewhat limited, this approach would allow very precise targeting within tissues[36].

Our current study characterizes the use of light-activated MNM **1** as an effective nanomechanical antibacterial agent against extensively-drug-resistant *K. pneumoniae.* In addition to its ability to counter antibacterial resistance, light-activated MNM **1** has several potential therapeutic applications. It can be used to treat skin infections, wound infections and urinary tract infections caused by many pathogens due to its broad-spectrum activity. Light-activated MNM **1**

has the potential to disrupt biofilms on indwelling prosthetic devices thereby allowing the antibiotic treatment to be more efficacious against biofilm forming pathogens.

Conclusions

In this study, we show that light-activated MNM **1** display antibacterial properties against *K. pneumoniae* that is not diminished even in an extensively drug resistant strain (Figure 3). This is because bacterial antimicrobial resistance mechanisms are not developed against a nanomechanical agent that disrupts bacterial cell walls. We have shown the ability of light-activated MNM **1** to disrupt cell walls by its nanomechanical action; using *K. pneumoniae* cell wall IM and OM permeability assays (Figure 4 and 5). The ability to use nanomechanical force to disrupt bacterial cell walls is a unique feature of MNM with the potential of many therapeutic applications and has not been characterized before. With only 5 min of MNM **1** light-activation, we observed 14 – 17% in viability reduction of *K. pneumoniae.* Next we show that light-activated MNM **1** can combine with meropenem at sub-therapeutic concentrations to be effective against an extensively-drug-resistant *K. pneumoniae* strain (Figure 6). The ability to help otherwise ineffective antibiotics to be efficacious is another unique aspect of light-activated MNM **1**. The use of MNM **1** in combination with other conventional antibiotic allows the potential recycling of many currently available antibiotics against MDR pathogens.

Methods

Bacterial strains. Two clinical strains of *K. pneumoniae* were used. An extensively drug-resistant *K. pneumonia*, AR-0666 (ψkp6) obtained from the CDC and a KPC-negative antibiotic sensitive strain, NIH-1 (ψkp7) obtained from the National Institutes of Health (NIH).

Synthesis of Molecular Machines. The molecular motors **1** and **2** were freshly prepared according to our previous protocols.[17, 36] The molecular motor **3** is new-designed and synthesized as described in the Supplementary Information.

Molecular nanomachines (MNM). MNM **1** is a fast motor with a rotor that rotates at 2-3 x 10^6 revolutions per second relative to its stator (Figure 1 b). MNM **2** is a slow motor that rotates about 1.8 revolutions per hour (Figure 1 c). MNM **2** served as a negative control. MNM **3** is MNM **1** attached to triphenylphosphonium (TPP) cation at the stator (Figure 1 d). TPP targets eukaryotic mitochondria and was used to demonstrate eukaryotic cell targeting of MNM.

Minimal inhibitory concentration (MIC) and minimal bactericidal concentration (MBC_{99}) of antibiotics in *K. pneumoniae*. Log-phase *K. pneumoniae* cultures (4-5 x 10^5 CFU/mL) grown in Mueller-Hinton broth (MHB) were exposed to antibiotics for 16 h in 96-well plates in triplicates. 1:2 serial dilutions of each antibiotic were assays in a microdilution assay against K. pneumoniae. Perkin Elmer EnVision microplate reader was used to measure culture optical density (OD) at 600 nm. After antibiotic exposure, bacterial cultures were plated for CFL/mL counts. The MIC and MBC_{99} values were calculated relative to the starting CFU/mL. MIC was defined as the minimal concentration of antibiotic needed to inhibit the growth of the starting culture of bacteria (≤100%). MBC_{99} was defined as the minimal concentration of the antibiotic needed to kill 99% of the starting culture of bacteria (≤1%).

***K. pneumoniae* viability reduction assay.** Log-phase *K. pneumoniae* cultures (2-4 x 10^5 CFU/mL) grown in Lysogeny broth (LB) were exposed to MNM in triplicates. The concentration of MNM used was 10 μM in 0.1% DMSO *K. pneumoniae* cultures were incubated with MNM for 30 minutes prior to 5 min of 365 nm light-activation. 365 nm light source was placed directly

above the cultures at a constant distance of 1.3 cm (Figure 1 d). After light exposure, bacterial cultures were plated for CFL/mL counts.

Inner membrane permeability assay. *K. pneumoniae* (2-4 x 10^5 CFU/mL) was washed once with 10 mM sodium phosphate (pH 7.4) and resuspended in the same buffer containing 1.5 mM ortho-nitrophenyl-β-galactoside (ONPG).[24] Cultures were incubated with 10 μM MNM in a black 96-well plate with clear bottoms with 100 μL of *K. pneumoniae* in four replicates. MNM were light-activated for 5 min with the light source placed directly above the 96-well plate (Figure 2 e). The production of o-nitrophenol was monitored at an absorbance of 410 nm every 3 min for 45 min post-light-exposure. Miller calculation was used to determine the inner membrane permeability.

Outer membrane permeability assay. *K. pneumoniae* (2-4 x 10^5 CFU/mL, 100 μL) was incubated with 10 μM MNM in a black 96-well plate with clear bottoms for 30 min and then light-activated for 5 min, in 4 replicates (Figure 2 e). After light-activation, 10 mM 1-N-phenylnaphthylamine (NPN) was mixed and incubated for 30 min. The fluorescence intensity due to the partitioning of NPN into the OM was measured with a microplate reader fluorescence spectrophotometer with an excitation wavelength of 350 nm and an emission wavelength of 430 nm.

Cell membrane integrity assay. Similar to the OM permeability assay, *K. pneumoniae* was exposed to MNM and light-activated for 5 min in 4 replicates. These cultures were spun down at 10,000 rpm and the supernatant was placed in a 96-well plate. The release of cytoplasmic constituents of the cell was monitored using the absorbance at 260 nm.[26]

MNM and meropenem combined assay. Similar to viability reduction assays, ψkp6 cultures (2-4 x 10^5 CFU/mL) were incubated with 10 μM of MNM and meropenem for 30 min

and activated with 365 nm light for 5 min in triplicates. Different concentrations of meropenem (0,5, 4, 16, and 64 µg/mL) was used with 10 µM of MNM. Tetracycline (16 and 128 µg/mL) was used as an antibiotic control with MNM. These cultures were then plated for CFU/mL counts.

Transmission electron microscopy (TEM). Log-phase ψkp6 (5 x 10^6 CFU/mL) were exposed to 10 µM of MNM **1** and 4 µg/mL of meropenem with and without light-activation for TEM. The four exposure groups were: (a) MNM **1** only, without light-activation, (b) MNM **1** only, with light-activation, (c) MNM **1** with meropenem, without light-activation and (d) MNM **1** with meropenem, with light-activation. Post-exposure, *K. pneumoniae* was incubated with meropenem for an additional 2 h. Then they were fixed with 4% formaldehyde, 2.5% glutaraldehyde and 1% acrolein. After 3x washes, they were embedded in Epon 812 resin and stained with 5% uranyl acetate. The embedded samples will be sectioned into grids and imaged with JEOL 1200 TEM. Cell wall disruptions, cytoplasmic clearance, cytoplasmic leakage, and bacterial elongation were quantified using 60-80 ψkp6 for each group.

Macrophage cytotoxic assay. A lactate dehydrogenase (LDH) cytotoxicity colorimetric assay kit (Biovision, #K311) was used to measure the cytotoxicity of MNM at different concentrations (0.5, 1, 10, 50 and 100 µM) in a J774A.1 macrophage cell line. J774A.1 cells (5 x 10^5 cells/mL) grown in DMEM media with 10% FBS were incubated with MNM in a 96-well plate (100 µL in each well) and exposed to 5 min of 365 nm light (Figure 2 f, 8 and d). Cytotoxicity of MNM with and without light activation was measured at 0.5, 4 and 24 h post exposure. DMSO and MNM **2** were used as negative controls. MNM **3** was used as a cell targeted positive control.

Statistical analyses. All experiments were done with at least three replicates ($n \geq 3$). The number of replicates used in each experiment is stated in the figure legend of each experiment. Prism GraphPad was used to perform two-tailed unpaired Student t-test statistical analyzes to

compare the means of two exposure groups. For comparison among 3 or more groups, analysis of variance (ANOVA) was used. A Mann–Whitney U test was used to compare different survival plots. Means and standard errors are presented in each of the graphs plotted in Microsoft Excel. $P < 0.05$ was defined as statistically significant.

Acknowledgments

This work was supported in part by grants from the Discovery Institute, the Welch Foundation, NIH R01 grant AI104960, BBSRC, and the Royal Society University Research Fellowship. We thank Drs. Dustin K. James and Preeti Sule for help coordinating this work, Dr. Riti Sharan for her assistance in antibiotic MIC assays in *K. pneumoniae* strains, Dr. Kristen Maitland for help with characterizing the light source, and Dr. Stanislav Vitha and Richard Littleton at the Texas A&M University Microscopy Imaging Center (MIC) for assistance with transmission electron microscopy (TEM).

Supporting Information Available.

Synthesis information is available as supplementary information. This material is available free of charge via the internet at http://pubs.acs.org.

REFERENCES

1. O'Neill, J., Tackling drug-resistant infections globally: final report and recommendations. *Review on Antimicrobial Resistance* **2016**, 1-84.

2. Brown, E. D.; Wright, G. D., Antibacterial drug discovery in the resistance era. *Nature* **2016,** *529* (7586), 336-43.

3. CDC, Antibiotic Resistant Threats in the United States. *Centers for Disease Control and Prevention* **2013**.

4. WHO, Global action plan on antimicrobial resistance. *World Health Organization* **2015**.

5. WHO, WHO priority pathogens list for R&D of new antibiotics. *World Health Organization* **2017**.

6. Han, J. H.; Goldstein, E. J.; Wise, J.; Bilker, W. B.; Tolomeo, P.; Lautenbach, E., Epidemiology of Carbapenem-Resistant Klebsiella pneumoniae in a Network of Long-Term Acute Care Hospitals. *Clin Infect Dis* **2017,** *64* (7), 839-844.

7. Gorrie, C. L.; Mirceta, M.; Wick, R. R.; Edwards, D. J.; Thomson, N. R.; Strugnell, R. A.; Pratt, N. F.; Garlick, J. S.; Watson, K. M.; Pilcher, D. V.; McGloughlin, S. A.; Spelman, D. W.; Jenney, A. W. J.; Holt, K. E., Gastrointestinal Carriage Is a Major Reservoir of Klebsiella pneumoniae Infection in Intensive Care Patients. *Clin Infect Dis* **2017,** *65* (2), 208-215.

8. CDC, Klebsiella pneumoniae in Healthcare Settings. *Centers for Disease Control and Prevention* **2012**.

9. Gomez-Simmonds, A.; Uhlemann, A. C., Clinical Implications of Genomic Adaptation and Evolution of Carbapenem-Resistant Klebsiella pneumoniae. *J Infect Dis* **2017,** *215* (suppl_1), S18-s27.

10. Chung, P. Y., The emerging problems of Klebsiella pneumoniae infections: carbapenem resistance and biofilm formation. *FEMS Microbiol Lett* **2016,** *363* (20).

11. Hauck, C.; Cober, E.; Richter, S. S.; Perez, F.; Salata, R. A.; Kalayjian, R. C.; Watkins, R. R.; Scalera, N. M.; Doi, Y.; Kaye, K. S.; Evans, S.; Fowler, V. G., Jr.; Bonomo, R. A.; van Duin, D., Spectrum of excess mortality due to carbapenem-resistant Klebsiella pneumoniae infections. *Clin Microbiol Infect* **2016,** *22* (6), 513-9.

12. Munoz-Price, L. S.; Poirel, L.; Bonomo, R. A.; Schwaber, M. J.; Daikos, G. L.; Cormican, M.; Cornaglia, G.; Garau, J.; Gniadkowski, M.; Hayden, M. K.; Kumarasamy, K.; Livermore, D. M.; Maya, J. J.; Nordmann, P.; Patel, J. B.; Paterson, D. L.; Pitout, J.; Villegas, M. V.; Wang, H.; Woodford, N.; Quinn, J. P., Clinical epidemiology of the global expansion of Klebsiella pneumoniae carbapenemases. *Lancet Infect Dis* **2013,** *13* (9), 785-96.

13. Capone, A.; Giannella, M.; Fortini, D.; Giordano, A.; Meledandri, M.; Ballardini, M.; Venditti, M.; Bordi, E.; Capozzi, D.; Balice, M. P.; Tarasi, A.; Parisi, G.; Lappa, A.; Carattoli, A.; Petrosillo, N., High rate of colistin resistance among patients with carbapenem-resistant Klebsiella pneumoniae infection accounts for an excess of mortality. *Clin Microbiol Infect* **2013,** *19* (1), E23-e30.

14. Watson, M. A.; Cockroft, S. L., Man-made molecular machines: membrane bound. *Chem Soc Rev* **2016,** *45* (22), 6118-6129.

15. Xu, T.; Gao, W.; Xu, L. P.; Zhang, X.; Wang, S., Fuel-Free Synthetic Micro-/Nanomachines. *Adv Mater* **2017,** *29* (9).

16. Garcia-Lopez, V.; Chiang, P. T.; Chen, F.; Ruan, G.; Marti, A. A.; Kolomeisky, A. B.; Wang, G.; Tour, J. M., Unimolecular Submersible Nanomachines. Synthesis, Actuation, and Monitoring. *Nano Lett* **2015,** *15* (12), 8229-39.

17. Garcia-Lopez, V.; Chen, F.; Nilewski, L. G.; Duret, G.; Aliyan, A.; Kolomeisky, A. B.; Robinson, J. T.; Wang, G.; Pal, R.; Tour, J. M., Molecular machines open cell membranes. *Nature* **2017,** *548* (7669), 567-572.

18. Zielonka, J.; Joseph, J.; Sikora, A.; Hardy, M.; Ouari, O.; Vasquez-Vivar, J.; Cheng, G.; Lopez, M.; Kalyanaraman, B., Mitochondria-Targeted Triphenylphosphonium-Based Compounds: Syntheses, Mechanisms of Action, and Therapeutic and Diagnostic Applications. *Chem Rev* **2017,** *117* (15), 10043-10120.

19. Yigit, H.; Queenan, A. M.; Anderson, G. J.; Domenech-Sanchez, A.; Biddle, J. W.; Steward, C. D.; Alberti, S.; Bush, K.; Tenover, F. C., Novel carbapenem-hydrolyzing beta-lactamase, KPC-1, from a

591 carbapenem-resistant strain of Klebsiella pneumoniae. *Antimicrob Agents Chemother* **2001,** *45* (4), 1151-
592 61.
593 20. Smith Moland, E.; Hanson, N. D.; Herrera, V. L.; Black, J. A.; Lockhart, T. J.; Hossain, A.;
594 Johnson, J. A.; Goering, R. V.; Thomson, K. S., Plasmid-mediated, carbapenem-hydrolysing beta-
595 lactamase, KPC-2, in Klebsiella pneumoniae isolates. *J Antimicrob Chemother* **2003,** *51* (3), 711-4.
596 21. Woodford, N.; Tierno, P. M., Jr.; Young, K.; Tysall, L.; Palepou, M. F.; Ward, E.; Painter, R.
597 E.; Suber, D. F.; Shungu, D.; Silver, L. L.; Inglima, K.; Kornblum, J.; Livermore, D. M., Outbreak of
598 Klebsiella pneumoniae producing a new carbapenem-hydrolyzing class A beta-lactamase, KPC-3, in a New
599 York Medical Center. *Antimicrob Agents Chemother* **2004,** *48* (12), 4793-9.
600 22. Livermore, D. M., Has the era of untreatable infections arrived? *J Antimicrob Chemother* **2009,** *64*
601 *Suppl 1*, i29-36.
602 23. Doumith, M.; Ellington, M. J.; Livermore, D. M.; Woodford, N., Molecular mechanisms
603 disrupting porin expression in ertapenem-resistant Klebsiella and Enterobacter spp. clinical isolates from
604 the UK. *J Antimicrob Chemother* **2009,** *63* (4), 659-67.
605 24. Griffith, K. L.; Wolf, R. E., Jr., Measuring beta-galactosidase activity in bacteria: cell growth,
606 permeabilization, and enzyme assays in 96-well arrays. *Biochem Biophys Res Commun* **2002,** *290* (1), 397-
607 402.
608 25. Helander, I. M.; Mattila-Sandholm, T., Fluorometric assessment of gram-negative bacterial
609 permeabilization. *J Appl Microbiol* **2000,** *88* (2), 213-9.
610 26. Graca da Silveira, M.; Vitoria San Romao, M.; Loureiro-Dias, M. C.; Rombouts, F. M.; Abee,
611 T., Flow cytometric assessment of membrane integrity of ethanol-stressed Oenococcus oeni cells. *Appl*
612 *Environ Microbiol* **2002,** *68* (12), 6087-93.
613 27. Moellering, R. C., Jr.; Eliopoulos, G. M.; Sentochnik, D. E., The carbapenems: new broad
614 spectrum beta-lactam antibiotics. *J Antimicrob Chemother* **1989,** *24 Suppl A*, 1-7.

615 28. Domenech-Sanchez, A.; Martinez-Martinez, L.; Hernandez-Alles, S.; del Carmen Conejo, M.;
616 Pascual, A.; Tomas, J. M.; Alberti, S.; Benedi, V. J., Role of Klebsiella pneumoniae OmpK35 porin in
617 antimicrobial resistance. *Antimicrob Agents Chemother* **2003,** *47* (10), 3332-5.
618 29. Chopra, I.; Roberts, M., Tetracycline antibiotics: mode of action, applications, molecular biology,
619 and epidemiology of bacterial resistance. *Microbiol Mol Biol Rev* **2001,** *65* (2), 232-60 ; second page, table
620 of contents.
621 30. Veras, D. L.; Lopes, A. C.; da Silva, G. V.; Goncalves, G. G.; de Freitas, C. F.; de Lima, F. C.;
622 Maciel, M. A.; Feitosa, A. P.; Alves, L. C.; Brayner, F. A., Ultrastructural Changes in Clinical and
623 Microbiota Isolates of Klebsiella pneumoniae Carriers of Genes bla SHV, bla TEM, bla CTX-M, or bla
624 KPC When Subject to beta-Lactam Antibiotics. *ScientificWorldJournal* **2015,** *2015*, 572128.
625 31. Scavuzzi, A. M. L.; Alves, L. C.; Veras, D. L.; Brayner, F. A.; Lopes, A. C. S., Ultrastructural
626 changes caused by polymyxin B and meropenem in multiresistant Klebsiella pneumoniae carrying blaKPC-
627 2 gene. *J Med Microbiol* **2016,** *65* (12), 1370-1377.
628 32. Brown, L.; Wolf, J. M.; Prados-Rosales, R.; Casadevall, A., Through the wall: extracellular
629 vesicles in Gram-positive bacteria, mycobacteria and fungi. *Nat Rev Microbiol* **2015,** *13* (10), 620-30.
630 33. Sahly, H.; Keisari, Y.; Crouch, E.; Sharon, N.; Ofek, I., Recognition of bacterial surface
631 polysaccharides by lectins of the innate immune system and its contribution to defense against infection:
632 the case of pulmonary pathogens. *Infect Immun* **2008,** *76* (4), 1322-32.
633 34. Thomas, R.; Brooks, T., Common oligosaccharide moieties inhibit the adherence of typical and
634 atypical respiratory pathogens. *J Med Microbiol* **2004,** *53* (Pt 9), 833-40.
635 35. Krivan, H. C.; Roberts, D. D.; Ginsburg, V., Many pulmonary pathogenic bacteria bind specifically
636 to the carbohydrate sequence GalNAc beta 1-4Gal found in some glycolipids. *Proc Natl Acad Sci U S A*
637 **1988,** *85* (16), 6157-61.
638 36. Liu, D.; Garcia-Lopez, V.; Gunasekera, R. S.; Greer Nilewski, L.; Alemany, L. B.; Aliyan, A.;
639 Jin, T.; Wang, G.; Tour, J. M.; Pal, R., Near-Infrared Light Activates Molecular Nanomachines to Drill
640 into and Kill Cells. *ACS Nano* **2019,** *13* (6), 6813-6823.

641

ToC

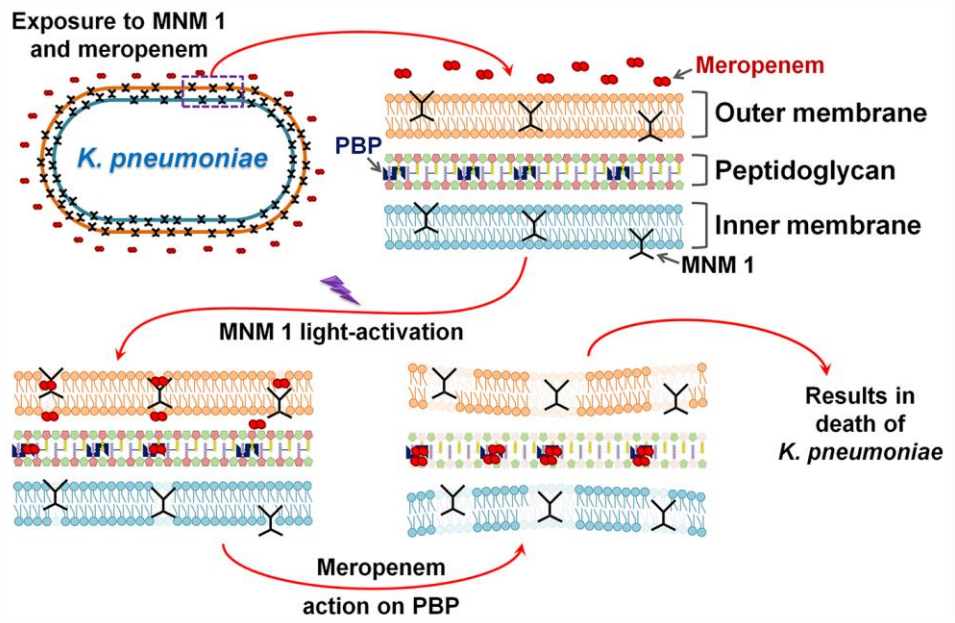

Model illustrating the combined action of molecular nanomachine (MNM) 1 nanomechanical action and meropenem on *K. pneumoniae*. A meropenem resistant *K. pneumoniae* exposed to sub-therapeutic concentrations meropenem (4 µg/mL) and MNM **1** has no reduction in bacterial viability. Meropenem is unable to reach its target sites within the periplasmic space, due to resistant mechanisms on the cell wall outer membrane. Light-activation of MNM **1** causes it to rotate vigorously and drill pores on the cell wall through its nanomechanical action. This allows meropenem to cross the outer membrane and display improved meropenem activity resulting in bactericidal effects. This synergistic mechanism between light-activated MNM **1** and meropenem allows sub-therapeutic concentrations of meropenem to kill a meropenem resistant, extensively drug-resistant *K. pneumoniae*.